NASA TECHNICAL NOTE

NASA TN D-6864

NASA TN D-6864

VIBRATION AND AERODYNAMIC BUCKLING EXPERIMENTS FOR BLUNT TRUNCATED CONICAL SHELLS WITH RING-SUPPORTED EDGES

by Robert Miserentino and Sidney C. Dixon

Langley Research Center
Hampton, Va. 23365

NATIONAL AERONAUTICS AND SPACE ADMINISTRATION • WASHINGTON, D. C. • SEPTEMBER 1972

1. Report No. NASA TN D-6864	2. Government Accession No.	3. Recipient's Catalog No.
4. Title and Subtitle VIBRATION AND AERODYNAMIC BUCKLING EXPERIMENTS FOR BLUNT TRUNCATED CONICAL SHELLS WITH RING-SUPPORTED EDGES		5. Report Date September 1972 6. Performing Organization Code
7. Author(s) Robert Miserentino and Sidney C. Dixon		8. Performing Organization Report No. L-8185
9. Performing Organization Name and Address NASA Langley Research Center Hampton, Va. 23365		10. Work Unit No. 502-32-04-80 11. Contract or Grant No.
12. Sponsoring Agency Name and Address National Aeronautics and Space Administration Washington, D.C. 20546		13. Type of Report and Period Covered Technical Note 14. Sponsoring Agency Code
15. Supplementary Notes		

16. Abstract

The vibration and buckling characteristics of a series of 140° ring-supported conical shells have been investigated experimentally and analytically. Experimental results were obtained from 14 conical shells, each attached to a solid nose cap at the small end. The large (base) end was either free or attached to a solid ring of rectangular cross section. The size of the solid base rings of rectangular cross section was systematically varied to provide a wide range of edge restraint. Shell buckling was induced by aerodynamic loading at a Mach number of 3; the vibration data were obtained prior to the wind-tunnel tests.

The experimental vibration data indicated that the size of the base rings had a pronounced effect on the magnitude of the frequencies and on the frequency spectrum. For vibration modes having less than two circumferential waves, the frequencies decreased with increasing ring size; whereas, for modes with several circumferential waves, the frequencies initially increased rapidly with ring size and then became relatively insensitive to further increases in ring size. This latter behavior was similar to the trend exhibited by the variation of buckling pressure with ring size. The experimental results were in excellent qualitative agreement with theoretical results and indicated that current shell-of-revolution analyses are adequate for predicting the vibration and buckling behavior of ring-supported shells, at least for the simple isotropic shells considered in this investigation.

17. Key Words (Suggested by Author(s)) Buckling Vibration Conical shells Ring-supported edges	18. Distribution Statement Unclassified – Unlimited		
19. Security Classif. (of this report) Unclassified	20. Security Classif. (of this page) Unclassified	21. No. of Pages 33	22. Price* $3.00

*For sale by the National Technical Information Service, Springfield, Virginia 22151

VIBRATION AND AERODYNAMIC BUCKLING EXPERIMENTS FOR BLUNT TRUNCATED CONICAL SHELLS WITH RING-SUPPORTED EDGES

By Robert Miserentino and Sidney C. Dixon
Langley Research Center

SUMMARY

The vibration and buckling characteristics of a series of 140° ring-supported conical shells have been investigated experimentally and analytically. Experimental results were obtained from 14 conical shells, each attached to a solid nose cap at the small end. The large (base) end was either free or attached to a solid ring of rectangular cross section. The size of the base rings was systematically varied to provide a wide range of edge restraint. Shell buckling was induced by aerodynamic loading at a Mach number of 3 in the Langley 9- by 6-foot thermal structures tunnel; the vibration data were obtained prior to the wind-tunnel tests.

The experimental vibration data indicated that the size of the base rings had a pronounced effect on the magnitude of the frequencies and on the frequency spectrum. For vibration modes having less than two circumferential waves, the frequencies decreased with increasing ring size; whereas, for modes with several circumferential waves, the frequencies initially increased rapidly with ring size and then became relatively insensitive to further increases in ring size. This latter behavior was similar to the trend exhibited by the variation of buckling pressure with ring size.

The experimental results were in excellent qualitative agreement with theoretical results and indicated that current shell-of-revolution analyses are adequate for predicting the vibration and buckling behavior of ring-supported shells, at least for the simple isotropic shells considered in the present investigation.

INTRODUCTION

Rings are often used to provide edge support for conical shells in a variety of aerospace configurations such as planetary entry vehicles and rocket nozzles. (See refs. 1 and 2.) Since such structures are subjected to both static and dynamic loading, a thorough knowledge of the vibration and buckling characteristics of ring-supported conical shells is needed. Recently, there have been several theoretical studies of the vibration and buckling

characteristics of ring-supported conical shells (refs. 1 to 9), but only a few configurations have been investigated experimentally (refs. 6 to 9). The available buckling results (ref. 7) were obtained from a preliminary wind-tunnel investigation of models that incurred large prebuckling deformations during tunnel startup. These deformations precluded a meaningful evaluation of available analytical methods.

The purpose of the present paper is to investigate the vibration characteristics of ring-supported cones and their buckling strength under aerodynamic loading. A series of 140° ring-supported conical shells is considered both experimentally and analytically. Experimental results were obtained from 14 conical shells, each attached to a solid nose cap at the small end. The large (base) end was either free or attached to a solid ring of rectangular cross section. The size of the base rings was systematically varied to provide a wide range of edge restraint. The vibration data were obtained prior to the wind-tunnel tests. The models were protected from the tunnel startup loads by a retractable support and received no observable prebuckling deformations. Shell buckling was induced by aerodynamic loading at a free-stream Mach number of 3 in the Langley 9- by 6-foot thermal structures tunnel. In the wind-tunnel tests, the shells were subjected to lateral external pressure, and static equilibrium was maintained by the axial force applied at the small end of the shell (solid nose cap) by the mounting sting. Such a combination of loads will be encountered by the Viking aeroshell. The experimental data are presented and compared with analytical results obtained from the shell-of-revolution computer program SALORS (ref. 10), which is based on Sanders' shell theory. In the buckling calculations, the effects of live pressure loading (a pressure load that remains normal to the surface), nonlinear prestress, and prebuckling displacements and rotations are considered.

SYMBOLS

The units used for the physical quantities of this paper are given both in the International System of Units (SI) and in the U.S. Customary Units. Measurements and calculations were made in the U.S. Customary Units. The appendix presents conversion factors for the units used herein.

A	cross-sectional area of base ring
b	width of base ring (see fig. 6)
d	depth of base ring (see fig. 1)
E	Young's modulus

f	frequency
h	wall thickness of shell
I_y, I_z, I_{yz}	centroid moments and products of inertia of ring cross section
J	torsional constant of ring cross section
M	meridional moment
N	meridional force resultant
n	number of circumferential full waves
p	uniform lateral external pressure
R_1, R_2	radii of conical frustum at small and large end, respectively
u,v,w	meridional, circumferential, and normal displacements of middle surface of conical frustum, respectively
y,z	orthogonal conical coordinates (see fig. 6)
z_o	eccentricity of ring centroidal axis measured from inside shell surface
β	numerical factor associated with torsional stiffness of solid rectangular cross sections (see fig. 6)
μ	Poisson's ratio of shell or base ring
ρ	density
ϕ	meridional slope of shell edge

EXPERIMENT

Models

The aluminum models were 140^o truncated conical shells with a radius ratio R_2/R_1 of 2.667. Fourteen models were tested, seven with a nominal ratio of the large-end radius

to thickness (R_2/h) equal to 167 and the other seven with R_2/h of 125. Construction details and model dimensions are given in figure 1, and material properties are given in table I. The nominal values of model wall thickness were 0.152 cm (0.060 in.) and 0.203 cm (0.080 in.); difference in measured and nominal values did not exceed ±0.008 cm (±0.003 in.).

The conical shells were carefully constructed using the following procedure:

The shell blanks (2024-T3 aluminum) were annealed once, placed on a 140° spinning die, spun down to the die, taken off, and heat treated to a T3-2 condition. The internal surface roughness was then removed and the shell replaced on the die, spun slightly to relieve warping, and finished with abrasive to remove surface imperfections and to polish down to the required thickness. Lastly, the hardness was checked.

The conical shell portion of each model was attached by 24 screws to a solid nose cap, and the nose cap was rigidly attached to a sting balance. The large end of the model was either free or attached to solid base rings (machined from 6061-T6 aluminum) of rectangular cross section which were riveted to the conical shells every 5° (72 around) with 0.318-cm-diameter (1/8-in.) 100° head 2117-T3 rivets. The rings were 1.58 cm (0.625 in.) wide and had various depths (see fig. 1) ranging from 0.318 cm (0.125 in.) to 2.54 cm (1.000 in.).

Test Technique

Vibration tests.- The models were sting mounted in the wind-tunnel test section (fig. 2) and were vibrated prior to the wind-tunnel tests. The models were excited with an air-jet shaker, which is described in reference 11. The exciting frequency was varied between 5 and 1500 Hz until an increased response indicated a natural frequency. The exciting force applied by the shaker was then increased, and a noncontacting inductance pickup was moved about the shell outer surface to locate the node lines and measure the vibration amplitudes. The frequency was determined by an electronic counter.

Buckling tests.- Buckling was induced by aerodynamic loading. The buckling tests were conducted at zero angle of attack in the Langley 9- by 6-foot thermal structures tunnel, which is a Mach 3 blowdown facility (see ref. 12) exhausting to the atmosphere. The tunnel stagnation-pressure operating range is from 345 to 1380 kN/m^2 (50 to 200 psia). The models were subjected to severe buffeting as the starting shock wave moved across the model during tunnel startup. In an effort to minimize this effect, the models were supported by a retractable support cone and support vanes during tunnel startup. Figure 2 is a photograph of the model in the test section prior to a test. Figure 2(a) shows the model in place, the sting, and the support; and figure 2(b) shows the

model support cone and vanes partially retracted. The tunnel was started at the minimum dynamic pressure of 71 kN/m^2 (1480 lbf/ft^2) with the retractable support cone and vanes firmly against the sting-mounted model. Once the flow was established, the support cone and vanes were retracted 3.8 cm (1.5 in.), and the dynamic pressure was then increased until buckling occurred. The stagnation temperature for all tests was 311 K (100^o F).

Each of the 14 models was tested once; the longest test lasted about 30 seconds. The tunnel conditions throughout the test section were monitored for each test.

For each model, there were measurements of three force components (axial force, yaw, and yawing moment) and a base pressure. The base pressure was used to assure a stable wake flow. These data, together with data from previous investigations, established that the cones were loaded by a symmetric conical flow field. Motion pictures were taken at 400 frames per second as the main means of identifying the instant of buckling and mode shape. Results presented in reference 13 indicated that the pressure on a 120^o cone varies smoothly along the cone meridian; maximum variation from the average pressure was of the order of 10 percent. In reference 7 it was shown that the use of the results of reference 13 in conjunction with the measured base pressures for a 120^o cone gave essentially the same values for the average external pressure as that obtained from axial-force measurements of the balance. Hence, in this investigation the external pressure p acting on the shell was assumed to be uniform and to be adequately given by the magnitude of the measured axial force divided by the total frontal area of the model.

For the aerodynamic buckling tests the models were exposed to both an external lateral pressure and a tensile axial force applied at the small end of the shell. Hence, the meridional stress in the models was tension and buckling was induced solely by circumferential compression.

RESULTS AND DISCUSSION

Vibration

Experimental results.- The measured resonant frequencies for the recorded modes (for the simplest observed wave pattern in the longitudinal direction) are given in table II and figures 3, 4, and 5. For models with an unsupported base (figs. 4(a) and 5(a)) or for the smallest base ring (figs. 4(b) and 5(b)), the frequency variation with wave number indicates a minimum value of $n = 3$. For all other models the minimum value occurs at $n = 2$, except for the thinner models with the two largest rings. These models (see figs. 4(f) and 4(g)) have a minimum frequency at $n = 1$ and an additional relative minimum value at $n = 5$. The phenomenon of relative minimum values of frequency for ring-supported shells has been observed in previous experimental investigations. (See, for

example, ref. 9.) The overall trends of the experimental data are similar to the trends exhibited by the results of reference 9 for ring-supported bases and by those of reference 14 for cantilevered conical shells with unsupported bases.

As can be seen in figure 3, for $n < 2$, increases in ring size resulted in decreases in frequency. Hence, for this range of n, the added ring mass had more effect than the edge restraint provided by the ring. For $n = 2$, increases in ring depth initially resulted in decreases in frequency, but further increases in ring size resulted in increases in model frequency. However, the frequencies for the models with the largest rings were still less than the frequencies for the models with no rings. For $n = 3$, the addition of the smallest ring considered reduced the frequency to a value below the case of no ring, but the model frequencies increased rapidly with further increases in ring depth. For $n > 3$, the model frequencies increased rapidly with increasing ring depth initially and then became relatively insensitive to further increases in ring size. The upper-limit value of frequency presumably corresponds to the model frequencies for both ends clamped, but no experimental data were obtained to verify this assumption.

Comparison with theoretical results.- Theoretical and experimental variations of frequency with wave number n are shown in figures 4 and 5. The theoretical results were obtained from the shell-of-revolution computer program SALORS (ref. 10), which is based on Sanders' shell theory. The analysis accounts for the stiffness and inertia characteristics of the base rings in the shell boundary conditions. For all vibration calculations, 102 finite difference stations were used to define the mathematical model, which is shown in figure 6; also shown are expressions used to define the base-ring properties needed for the calculations. Theoretical results which were calculated for each value of n are presented as faired curves for both clamped and simple-support boundary conditions at the small end of the shells. For the clamped boundary conditions ($u = v = w = \phi = 0$), the radius at the small end of the shell was taken to be 9.525 cm (3.75 in.), which corresponds to the edge of the solid nose cap (see fig. 1); these results are indicated by the solid curves in figures 4 and 5. For the simple-support conditions ($N = v = w = M = 0$), the radius at the small end of the shell was taken to be 8.89 cm (3.50 in.), which corresponds to the downstream row of screws used to attach the models to the solid nose cap (see fig. 1); these results are indicated by the dashed curves in figures 4 and 5. As can be seen, the results for these two sets of boundary conditions differ considerably for $n \leqq 2$. However, for $n > 2$, the difference decreases and the results become essentially identical for $n \geqq 8$.

The qualitative agreement between theoretical and experimental results is excellent. For $n < 3$, the experimental data are bracketed by the two theoretical curves, but correlate better with the results calculated for a clamped condition at the small end of the shell. For the $n < 3$ range, the difference between the experimental and theoretical

results (for a clamped boundary condition) ranged from 0.5 percent to 66 percent. The quantitative agreement for $n \geq 3$ is good, with an average difference of about 7 percent between experimental and theoretical results for a clamped condition at the small end of the shell. One factor contributing to the difference in theoretical and experimental results is the use of nominal wall thickness in the calculations rather than accounting for the variations in measured wall thickness. Also, the theoretical frequencies are sensitive to the values of shell radii and length and location of the ring centroid, and slight variations in the values of these parameters (the values used are given in fig. 6) could alter the comparison of theoretical and experimental results somewhat. In addition, a precise modeling of the nose cap as a ring would probably result in a better correlation of results, particularly for $n \leq 3$, but such detailed calculations were not made.

Theoretical and experimental variations of frequency with base-ring depth d are shown in figure 7 for $n = 2$ and $n = 5$; the theoretical results are for a clamped boundary condition at the small end of the shell and ring support (solid and dashed curves) or a clamped boundary (solid symbols) at the large end of the shell. For $n = 5$, the frequency approaches an upper limit that differs from theoretical results from clamped edge support at both ends of the shell (the solid symbol) by about 10 percent. Hence, from figures 3 and 7 it appears that for $n \geq 4$ the frequencies approach the value for clamped support at both ends as the base-ring depth is increased to 2.54 cm (1.0 in.). Note that for $n = 2$ the experimental results for ring support even for the largest ring are about a factor of six less than the theoretical results for both ends clamped. Hence, a substantial increase in base-ring size (and mass) is required to effect a significant increase in the frequency of ring-supported shells for low values of the circumferential number n.

Typical effects of base rings on the vibration mode shapes are indicated in figure 8 where theoretical and experimental results for $n = 5$ for the thicker shells are shown. For the large end free or supported by the smaller rings, the maximum amplitude occurs at the large end, and the theoretical and experimental results are in excellent qualitative agreement but only fair quantitative agreement. As the size of the base ring is increased, the position of maximum amplitude moves from the large end toward the middle of the shell, the amplitude at the large end approaches zero, and both the qualitative and quantitative agreement between theoretical and experimental results becomes excellent.

Buckling

Experimental results.- During the wind-tunnel tests the shell models were monitored by closed-circuit television. The onset of buckling was accompanied by growing permanent deformations of the shell which caused changes in the light reflection pattern on the model. Observation of the changes in reflection pattern permitted the tunnel to be operated at pressures that never exceeded 120 percent of the shell buckling pressure.

The permanent deformations did not appear to change modes even during tunnel shutdown. After each test the model was examined to verify the buckle wave number. Motion-picture films taken during the test were viewed in order to establish the time of buckling and determine the buckling mode pattern. The time of buckling was verified by records of the axial force which showed a temporary unsteadiness in the ratio of axial force to tunnel pressure.

The buckling pressure (obtained from measured axial force) and circumferential wave number n are given in table III for each model. The models with smaller base rings buckled at lower values of pressure and smaller values of n as compared with the models having larger base rings. The thinner model with no base ring buckled into an $n = 5$ mode as soon as the support was retracted, and a reliable buckling pressure could not be established.

The thicker model with the largest base ring (d = 2.54 cm (1.00 in.)) withstood the maximum pressure loading obtainable in the tunnel without buckling; the model with the next largest ring (d = 1.91 cm (0.75 in.)) buckled at a pressure when the tunnel was just below the maximum obtainable pressure. For the two series of models (two nominal values of thickness), the buckling pressure initially increased rapidly with increasing ring depth and then became relatively insensitive to further increases in ring depth.

Comparison with theoretical results.- The theoretical and experimental variations of buckling pressure with ring depth are shown in figure 9. The calculated results were obtained from the computer program SALORS (ref. 10) and include the effects of live pressure loading, nonlinear prestress, and prebuckling displacements and rotations. For all buckling calculations, 401 finite difference stations were used to define the mathematical model, which is shown in figure 6; also shown are expressions used to define the base-ring properties needed for the calculations. The small end of the shell was assumed to be clamped for the buckling calculation. The agreement between the theoretical and experimental results is good, with the experimental results differing by from 4 percent to 26 percent of the theoretical values. This compares favorably with typical experimental data for static buckling of truncated conical shells subjected to lateral pressure loading, which range from 60 percent to 140 percent of the values predicted for simply supported edges (ref. 15). In reference 15 the higher experimental values were attributed to edge conditions being closer to clamped than the assumed simple support, and the lower values were attributed primarily to initial imperfections. For the present investigation the vibration results shown in figures 4 and 5 indicate that the edge restraints used in the theoretical calculations are adequate idealizations of the edge restraint actually imposed on the test models for $n \geq 3$. In addition, for the aerodynamic buckling tests of this investigation the meridional stress in the models was tension, and buckling was induced solely by circumferential compression, which should reduce the effects of initial imper-

fections. (See fig. 3 of ref. 16.) Also, the theoretical buckling pressures are sensitive to the values of shell radii and length and location of the ring centroid, and slight variations in the values of these parameters (the values used are given in fig. 6) could alter the comparison of theoretical and experimental results somewhat.

The theory is conservative for the models with smaller end rings and unconservative for the models with the larger end rings. Calculated results for both ends clamped are indicated by the solid symbols. The upper limit of the experimental data for the thinner models differs from the calculated value for clamped ends by less than 10 percent, which, as in the case for the vibration results of figure 7, suggests that the upper limits are essentially the values for the models with both ends clamped.

The data confirm the calculated trends of this and earlier investigations (for example, ref. 7) that if the base ring is not very stiff, a shell clamped at its small end buckles into very few circumferential waves (usually 3 or 4) at loads which vary considerably with ring size (stiffness). However, if the base ring is sufficiently stiff, the shell buckles into a higher number of circumferential waves at loads approaching the buckling loads for clamped edges; these loads do not vary significantly with ring size. Use of the smallest (lightest) ring required to achieve essentially the upper-limit buckling pressure generally results in minimum total mass of the shell and ring for a shell designed to withstand buckling. (See ref. 4.) The results of figure 9 suggest that current shell-of-revolution computer programs, such as SALORS, can adequately predict the required base-ring size for weight critical designs, at least for the simple isotropic shells considered in the present investigation.

CONCLUDING REMARKS

The vibration and buckling characteristics of ring-supported 140° conical shells have been investigated experimentally and theoretically. The conical shells were attached to solid nose caps at their small end and their large ends were unsupported (free) or supported by base rings. The size of the solid base rings was varied systematically to provide a wide range of edge restraint. Shell buckling was induced by aerodynamic loading in wind-tunnel tests conducted at Mach number 3; the vibration data were obtained prior to the wind-tunnel tests.

The experimental vibration results indicated that the size (mass and stiffness) of the base rings had a pronounced effect on the magnitude of the frequencies and on the frequency spectrum. For vibration modes having less than two circumferential waves, the frequencies decreased with increasing ring size; in contrast, for modes having several circumferential waves, the frequencies initially increased rapidly with increasing ring size and then became relatively insensitive to further increases in ring size. This latter

behavior was similar to the trend exhibited by the variation of buckling pressure with end-ring size.

The experimental results were in excellent qualitative agreement with theoretical trends. The quantitative agreement was good and indicated that current shell-of-revolution computer programs are adequate for predicting the vibration and buckling behavior of ring-supported shells, at least for the simple isotropic shells considered in the present investigation.

Langley Research Center,
National Aeronautics and Space Administration,
Hampton, Va., August 4, 1972.

APPENDIX

CONVERSION OF U.S. CUSTOMARY UNITS TO SI UNITS

Factors required for conversion of U.S. Customary Units to the International System (SI) are given in the following table:

Physical quantity	U.S. Customary Unit	Conversion factor (*)	SI Unit (**)
Area	in^2	0.6452×10^{-3}	$meters^2$ (m^2)
Length	in.	0.0254	meters (m)
Mass/Area	lbm/ft^2	4.882	$kilograms/meter^2$ (kg/m^2)
Mass density	lbm/in^3	2.768×10^4	$kilograms/meter^3$ (kg/m^3)
Moment of inertia	in^4	0.4162×10^{-6}	$meters^4$ (m^4)
Pressure	psi = lbf/in^2	6.895×10^3	$newtons/meter^2$ (N/m^2)
	lbf/ft^2	47.88	$newtons/meter^2$ (N/m^2)
Young's and shear moduli	lbf/in^2	6.895×10^3	$newtons/meter^2$ (N/m^2)
Temperature	^oF	$\frac{^oF + 459.67}{1.8}$	kelvins (K)

*Multiply value given in U.S. Customary Units by conversion factor to obtain equivalent value in SI Units.

**Prefixes to indicate multiples of units are as follows:

Prefix	Multiple
giga (G)	10^9
mega (M)	10^6
kilo (k)	10^3
centi (c)	10^{-2}
milli (m)	10^{-3}

REFERENCES

1. Cohen, Gerald A.: The Effect of Edge Constraint on the Buckling of Sandwich and Ring-Stiffened 120 Degree Conical Shells Subjected to External Pressure. NASA CR-795, 1967.

2. Newton, R. A.: Free Vibrations of Rocket Nozzles. AIAA J., vol. 4, no. 7, July 1966, pp. 1303-1305.

3. Almroth, B. O.; and Bushnell, D.: Computer Analysis of Various Shells of Revolution. AIAA J., vol. 6, no. 10, Oct. 1968, pp. 1848-1855.

4. Dixon, Sidney C.; and Carine, John B.: Preliminary Design Procedure for End Rings of Isotropic Conical Shells Loaded by External Pressure. NASA TN D-5980, 1970.

5. Cohen, Gerald A.; Foster, Richard M.; and Schafer, Everett M.: Analysis of Conceptual Designs for the Voyager Entry Capsule. Contract No. NAS 1-5554-1, Space & Re-Entry Systems Div., Philco-Ford Corp., [1968]. (Available as NASA CR-66580.)

6. Sewall, John L.; and Catherines, Donnell S.: Analytical Vibration Study of a Ring-Stiffened Conical Shell and Comparison With Experiment. NASA TN D-5663, 1970.

7. Dixon, Sidney C.; Miserentino, Robert; and Hudson, M. Latrelle: Theoretical and Experimental Vibration and Buckling Results for Blunt Truncated Conical Shells With Ring-Supported Edges. NASA TN D-7003, 1970.

8. Naumann, Eugene C.; and Mixson, John S.: Vibration Characteristics of Z-Ring-Stiffened 60° Conical Shell Models of a Planetary Entry Spacecraft. NASA TN D-6557, 1971.

9. Naumann, Eugene C.; Catherines, Donnell S.; and Walton, William C., Jr.: Analytical and Experimental Studies of Natural Vibration Modes of Ring-Stiffened Truncated-Cone Shells With Variable Theoretical Ring Fixity. NASA TN D-6473, 1971.

10. Anderson, M. S.; Fulton, R. E.; Heard, W. L., Jr.; and Walz, J. E.: Stress, Buckling, and Vibration Analysis of Shells of Revolution. Computers & Structures, vol. 1, nos. 1/2, Aug. 1971, pp. 157-192.

11. Herr, Robert W.: A Wide-Frequency-Range Air-Jet Shaker. NACA TN 4060, 1957.

12. Schaefer, William T., Jr.: Characteristics of Major Active Wind Tunnels at the Langley Research Center. NASA TM X-1130, 1965.

13. Stallings, Robert L., Jr.; and Tudor, Dorothy H.: Experimental Pressure Distributions on a 120° Cone at Mach Numbers From 2.96 to 4.63 and Angles of Attack From 0° to 20°. NASA TN D-5054, 1969.

14. Weingarten, Victor I.; and Gelman, Alfred P.: Free Vibrations of Cantilevered Conical Shells. J. Eng. Mech. Div., Amer. Soc. Civil Eng., vol. 93, no. EM 6, Dec. 1967, pp. 127-138.

15. Seide, Paul: A Survey of Buckling Theory and Experiment for Circular Conical Shells of Constant Thickness. Collected Papers on Instability of Shell Structures – 1962. NASA TN D-1510, 1962, pp. 401-426.

16. Budiansky, Bernard; and Amazigo, John C.: Initial Post-Buckling Behavior of Cylindrical Shells Under External Pressure. J. Math. & Phys., vol. 47, no. 3, Sept. 1968, pp. 223-235.

TABLE I.- MATERIAL PROPERTIES

Model components	Material	Young's modulus, E		Density, ρ		Poisson's ratio, μ
		GN/m^2	lbf/in^2	kg/m^3	lbm/in^3	
Ring	6061-T6 aluminum alloy	68.26	9.9×10^6	2768	0.1	0.32
Shell	2024-T3[-2] aluminum alloy	71.85	10.42×10^6	2768	0.1	0.32

TABLE II.- EXPERIMENTAL FREQUENCIES OF RING-SUPPORTED SHELLS

(a) h = 0.152 cm (0.060 in.)

n	f, Hz, for –						
	d = 0	d = 0.318 cm (0.125 in.)	d = 0.635 cm (0.250 in.)	d = 0.953 cm (0.375 in.)	d = 1.27 cm (0.500 in.)	d = 1.91 cm (0.750 in.)	d = 2.54 cm (1.00 in.)
0		1020	841	706	587	527	483
1	534	392	307	271	256	207	173
2	251	198	167	174	177	209	244
3	179	168	220	301	373	553	703
4	184	243	394	552	655	728	734
5	236	375	600	682	693	702	714
6	316	526	746	734	745	750	777
7	410	683	819	847	862	---	---
8	519	846	958	952	---	---	---
9	642	1014	---	---	---	---	---
10	777	1200	---	---	---	---	---

(b) h = 0.203 cm (0.080 in.)

n	f, Hz, for –						
	d = 0	d = 0.318 cm (0.125 in.)	d = 0.635 cm (0.250 in.)	d = 0.953 cm (0.375 in.)	d = 1.27 cm (0.500 in.)	d = 1.91 cm (0.750 in.)	d = 2.54 cm (1.00 in.)
2	267	220	198	178	198	212	249
3	212	198	243	305	384	535	702
4	241	268	425	563	684	759	822
5	328	404	625	795	839	790	860
6	446	582	866	906	931	910	985
7	585	776	996	1098	1122	1076	1157
8	743	1001	1222	----	----	1267	1373
9	918	----	----	1547	----	----	----

TABLE III.- EXPERIMENTAL BUCKLING PRESSURE FOR RING-SUPPORTED SHELLS

(a) h = 0.152 cm (0.060 in.)

d		n	p	
cm	in.		kN/m^2	lbf/in^2
0	0	5	-----	----
.318	.125	4	70.3	10.2
.635	.250	3	141.3	20.5
.953	.375	7	140.7	20.4
1.27	.500	7	155.1	22.5
1.91	.750	7	167.5	24.3
2.54	1.000	6	162.7	23.6

(b) h = 0.203 cm (0.080 in.)

d		n	p	
cm	in.		kN/m^2	lbf/in^2
0	0	4	77.2	11.2
.318	.125	4	135.1	19.6
.635	.250	3	275.1	39.9
.953	.375	7	339.2	49.2
1.27	.500	6	335.8	48.7
1.91	.750	8	342.0	49.6
2.54	1.000	-	-----	----

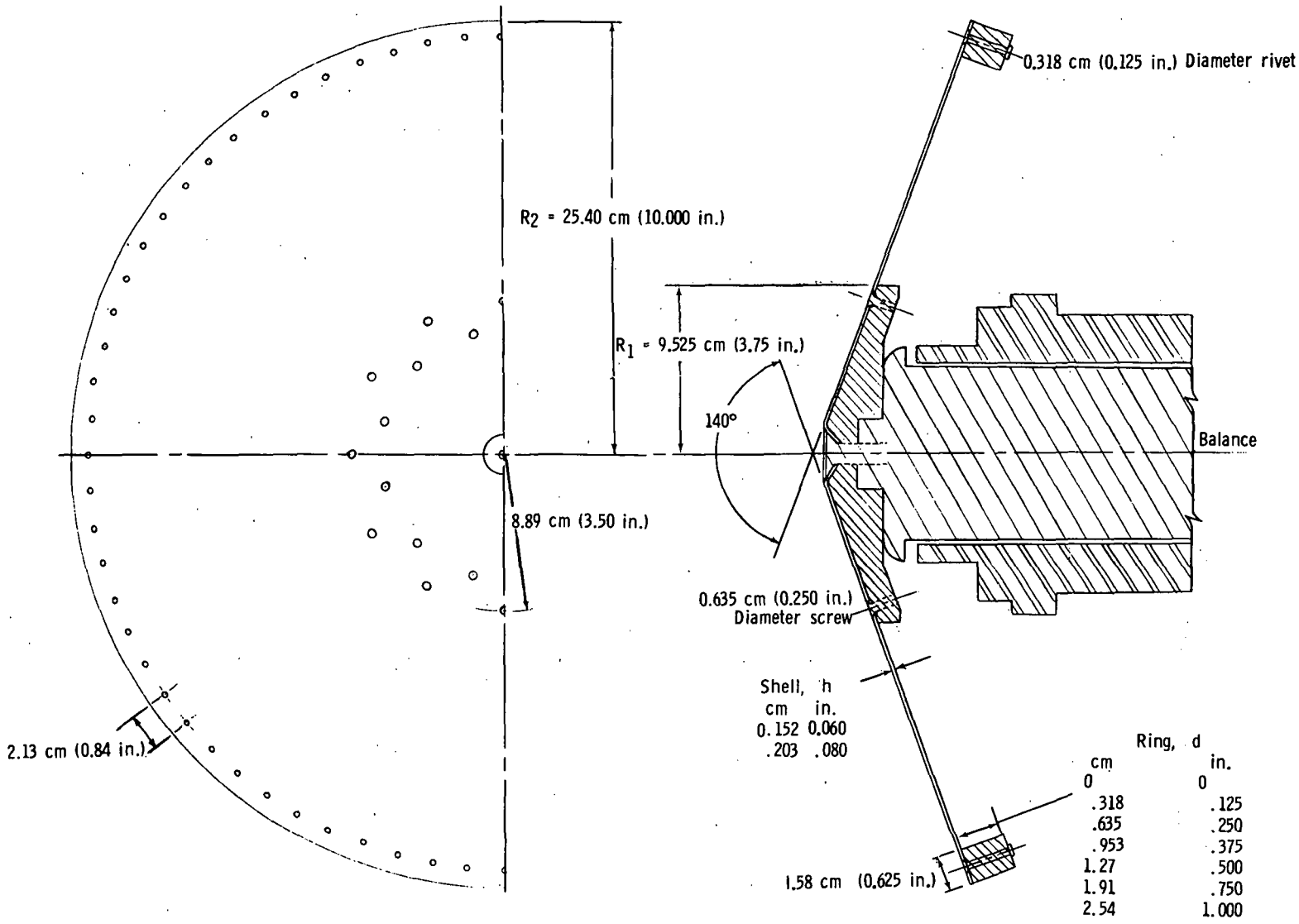

Figure 1.- Model dimensions.

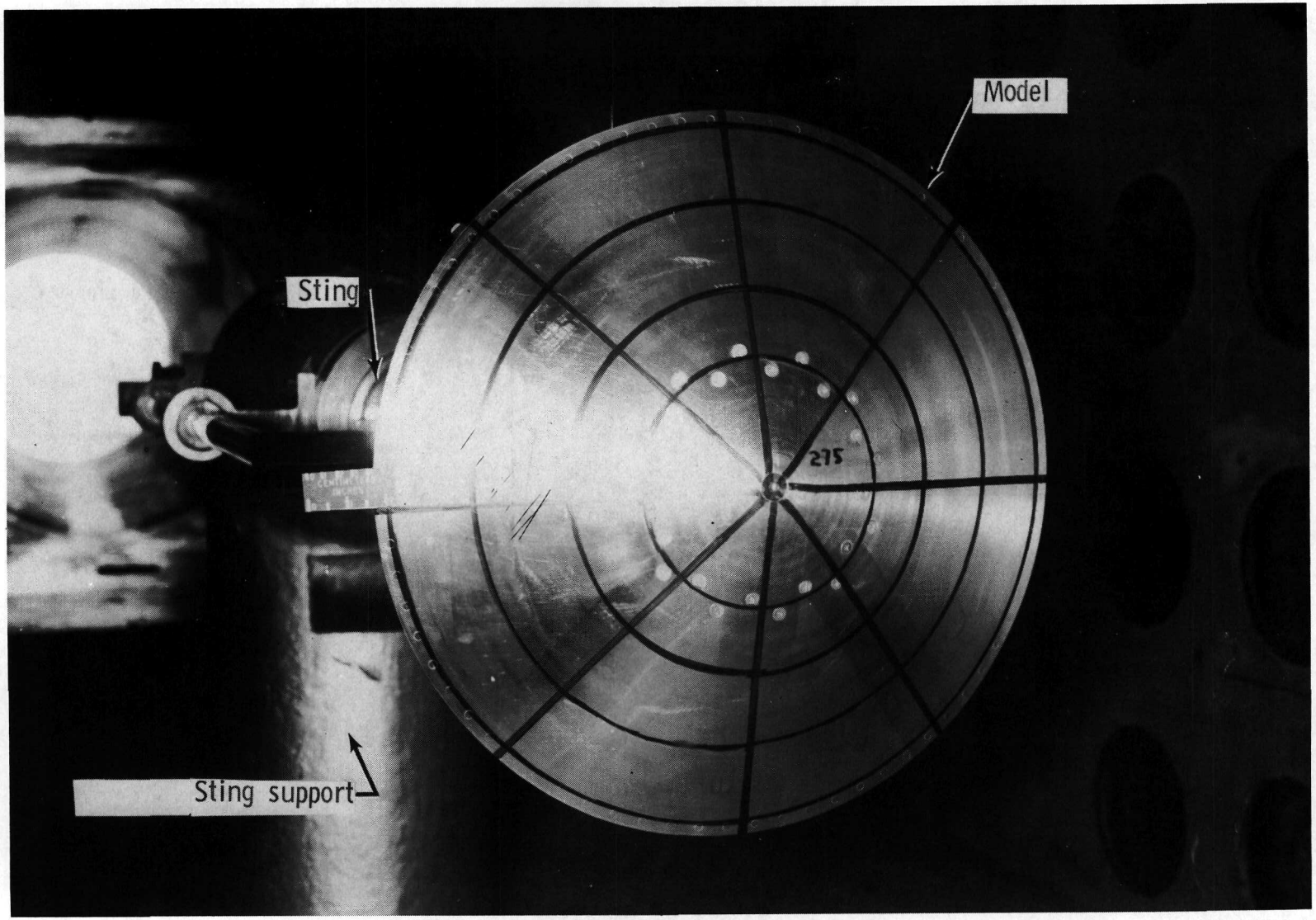

L-70-2316.1

(a) Forward face of conical shell.

Figure 2.- Model mounted in wind tunnel.

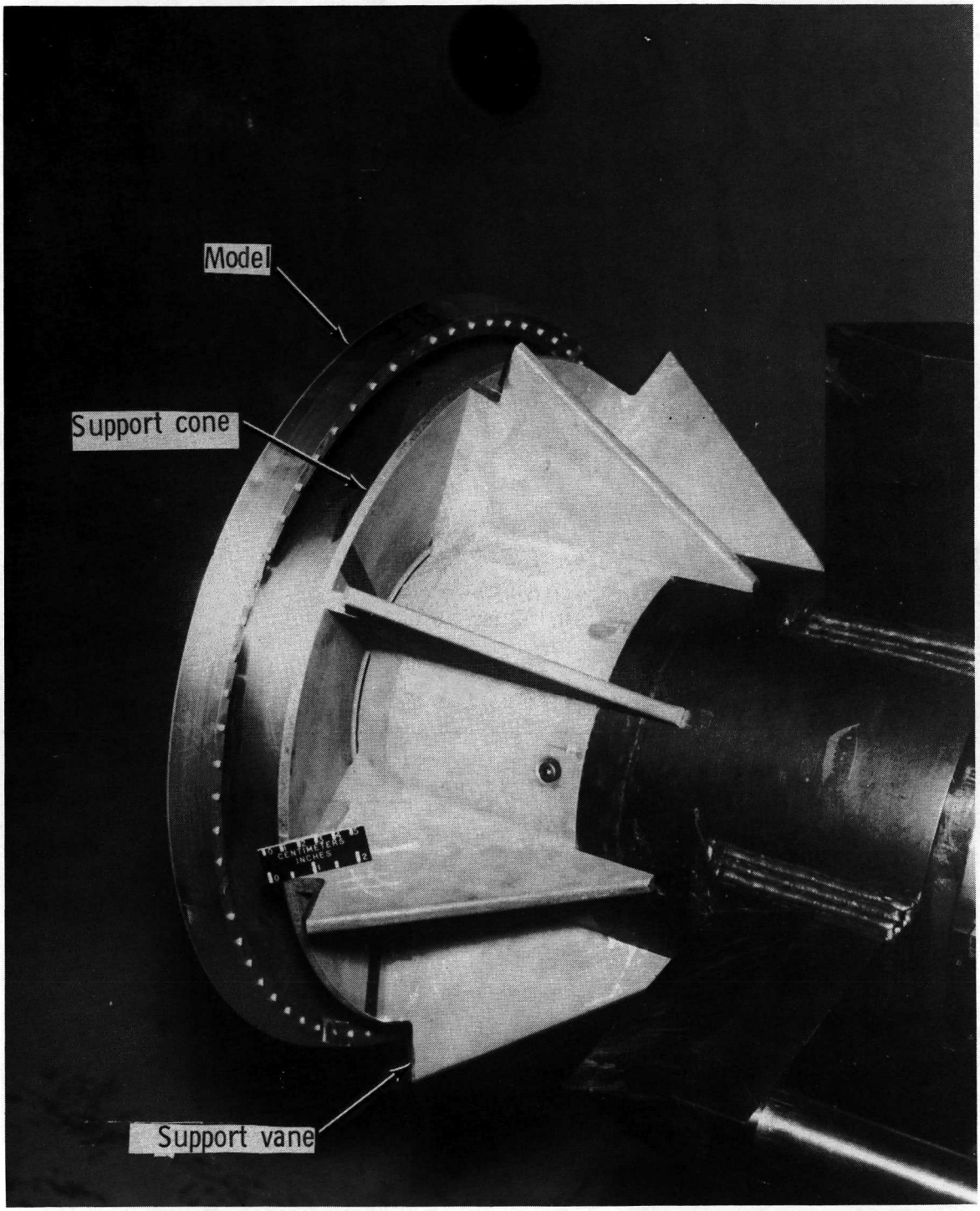

L-70-2312.1

(b) Aft edge of conical shell and retractable support.

Figure 2.- Concluded.

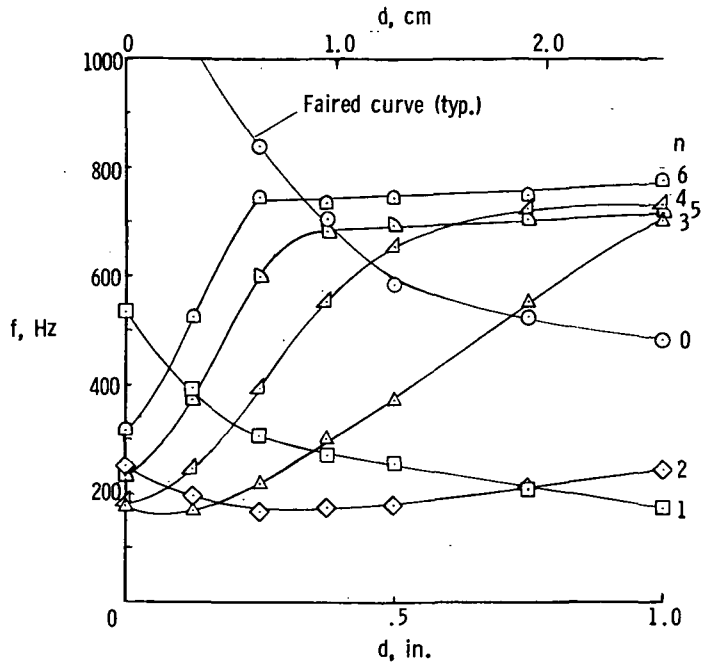

(a) h = 0.152 cm (0.060 in.).

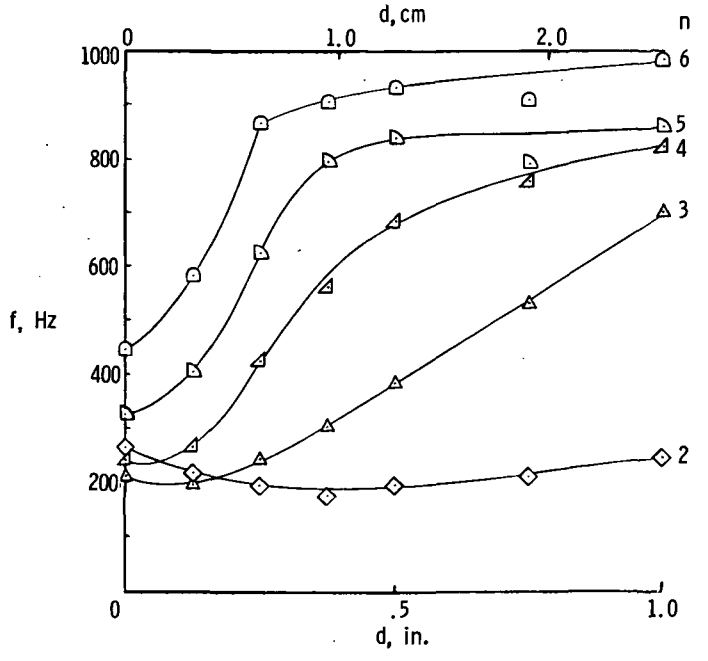

(b) h = 0.203 cm (0.080 in.).

Figure 3.- Variation of experimental frequencies with base-ring depth.

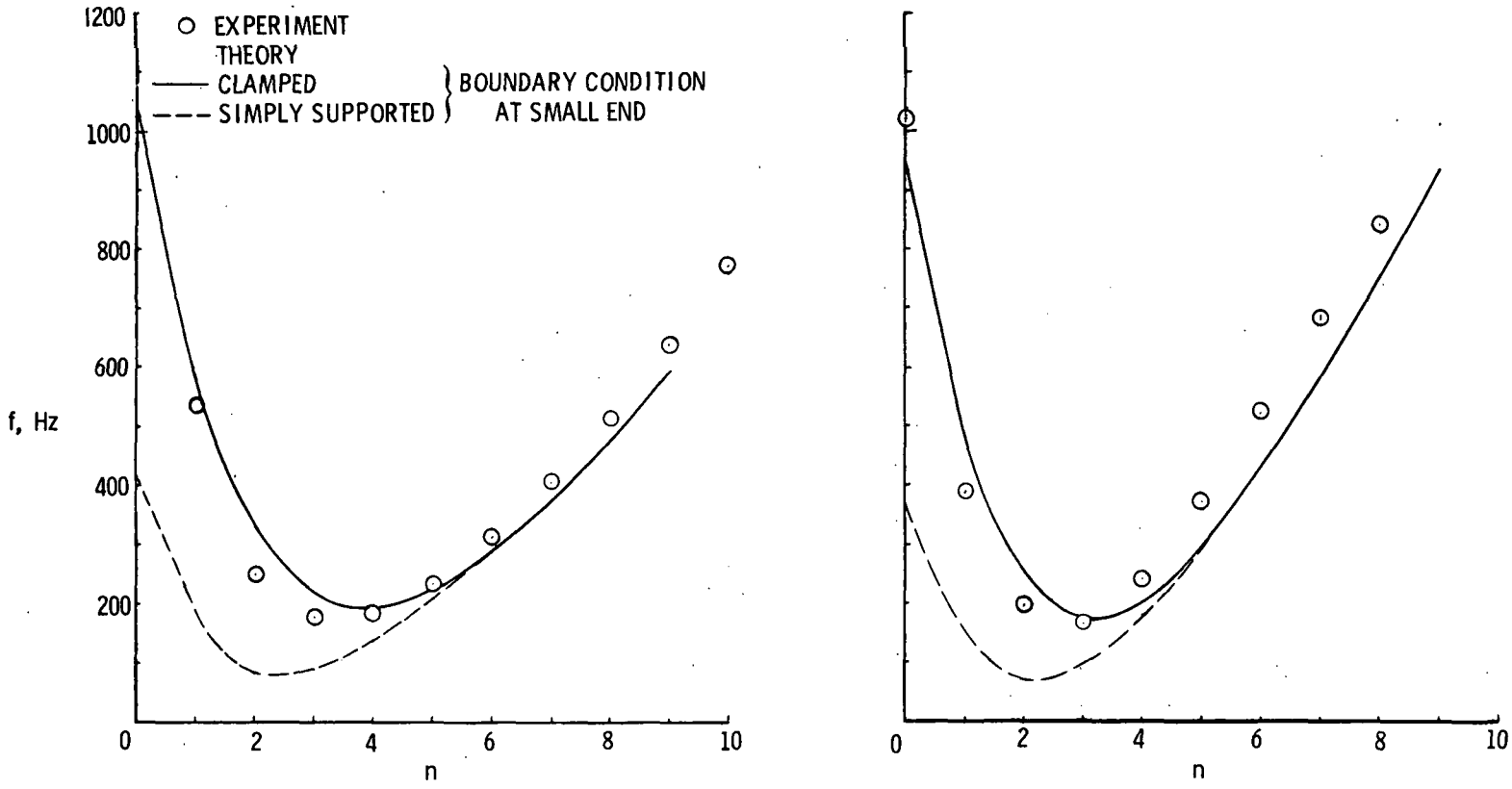

(a) No ring.

(b) d = 0.318 cm (0.125 in.).

Figure 4.- Experimental and theoretical frequencies of the 0.15-cm-thick (0.060-in.) shells.

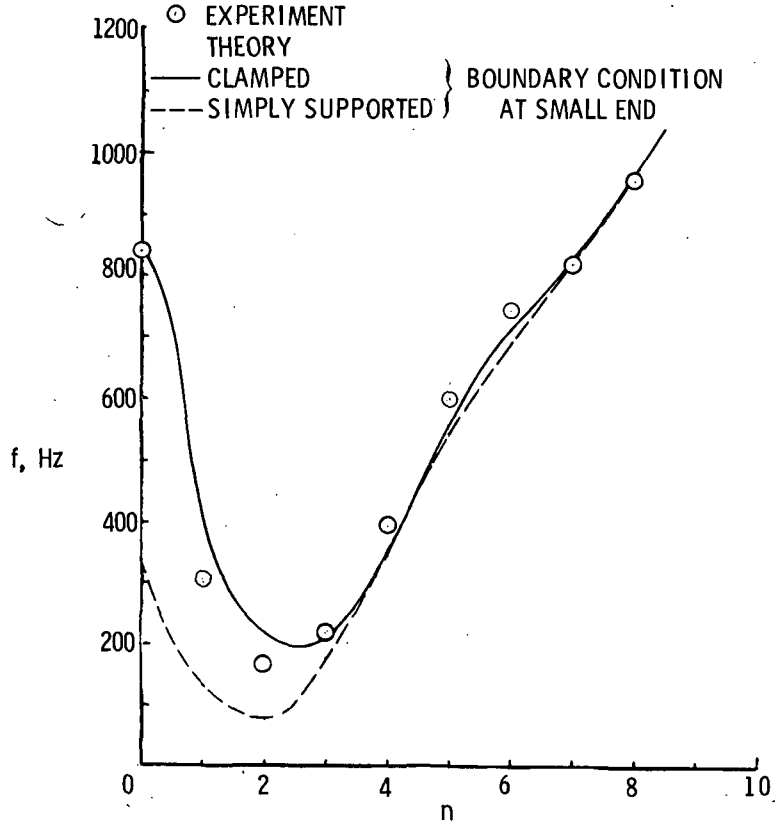

(c) d = 0.635 cm (0.250 in.).

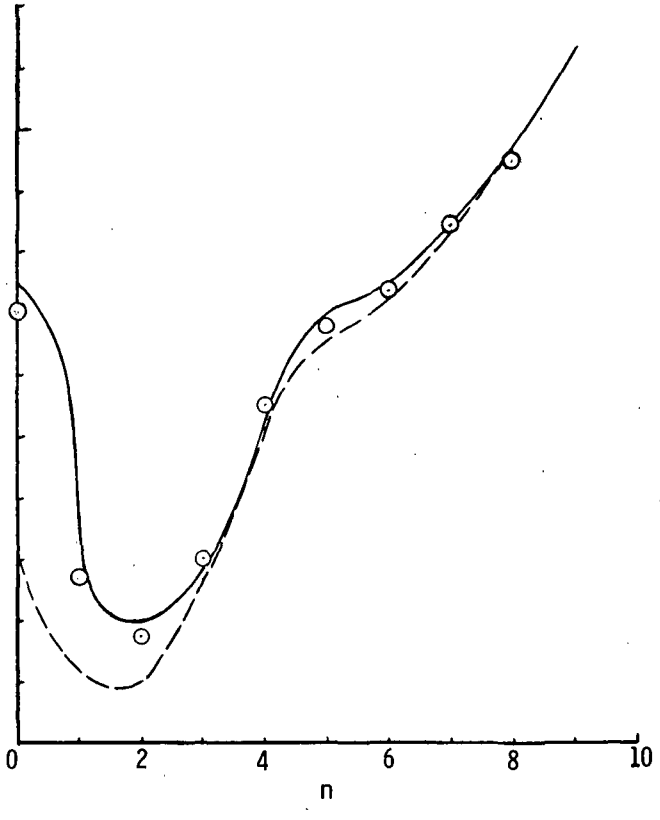

(d) d = 0.953 cm (0.375 in.).

Figure 4.- Continued.

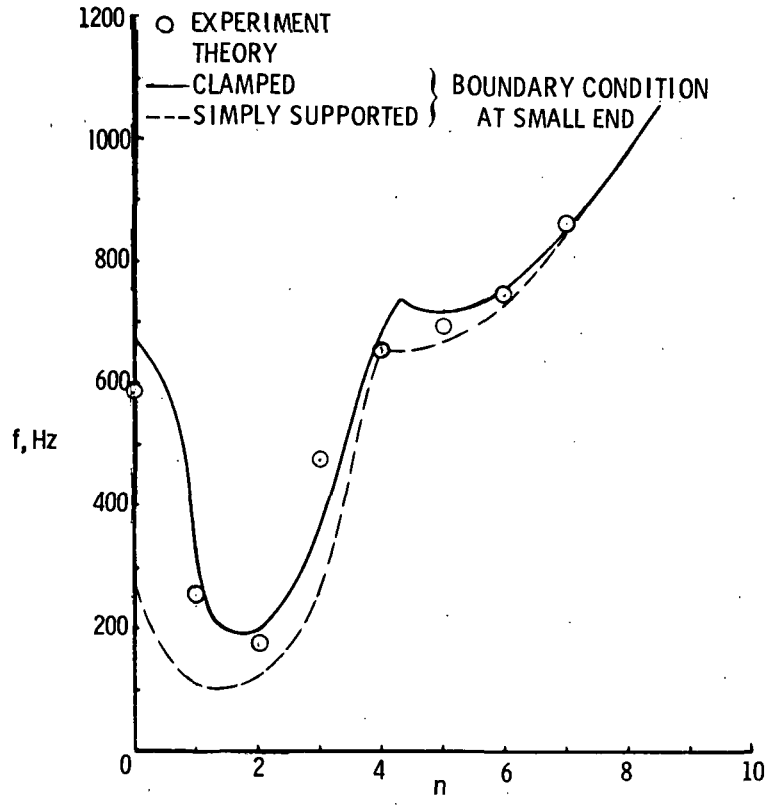

(e) d = 1.27 cm (0.500 in.).

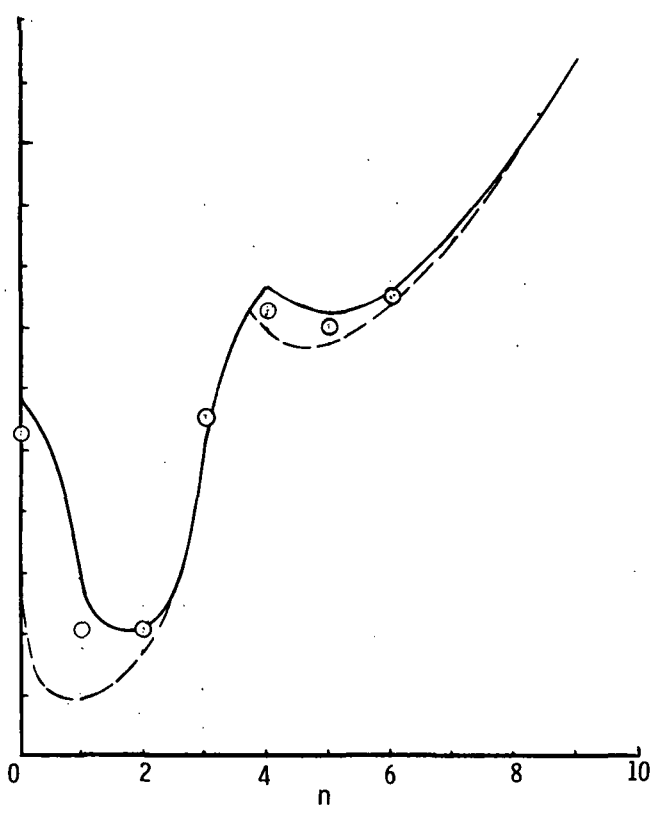

(f) d = 1.91 cm (0.750 in.).

Figure 4.- Continued.

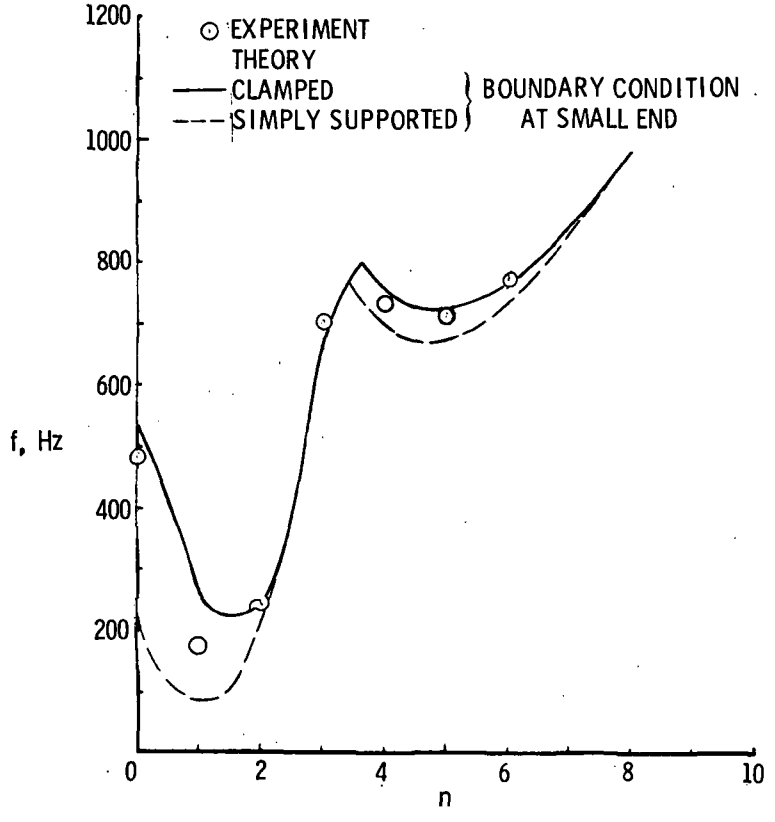

(g) d = 2.54 cm (1.000 in.).

Figure 4.- Concluded.

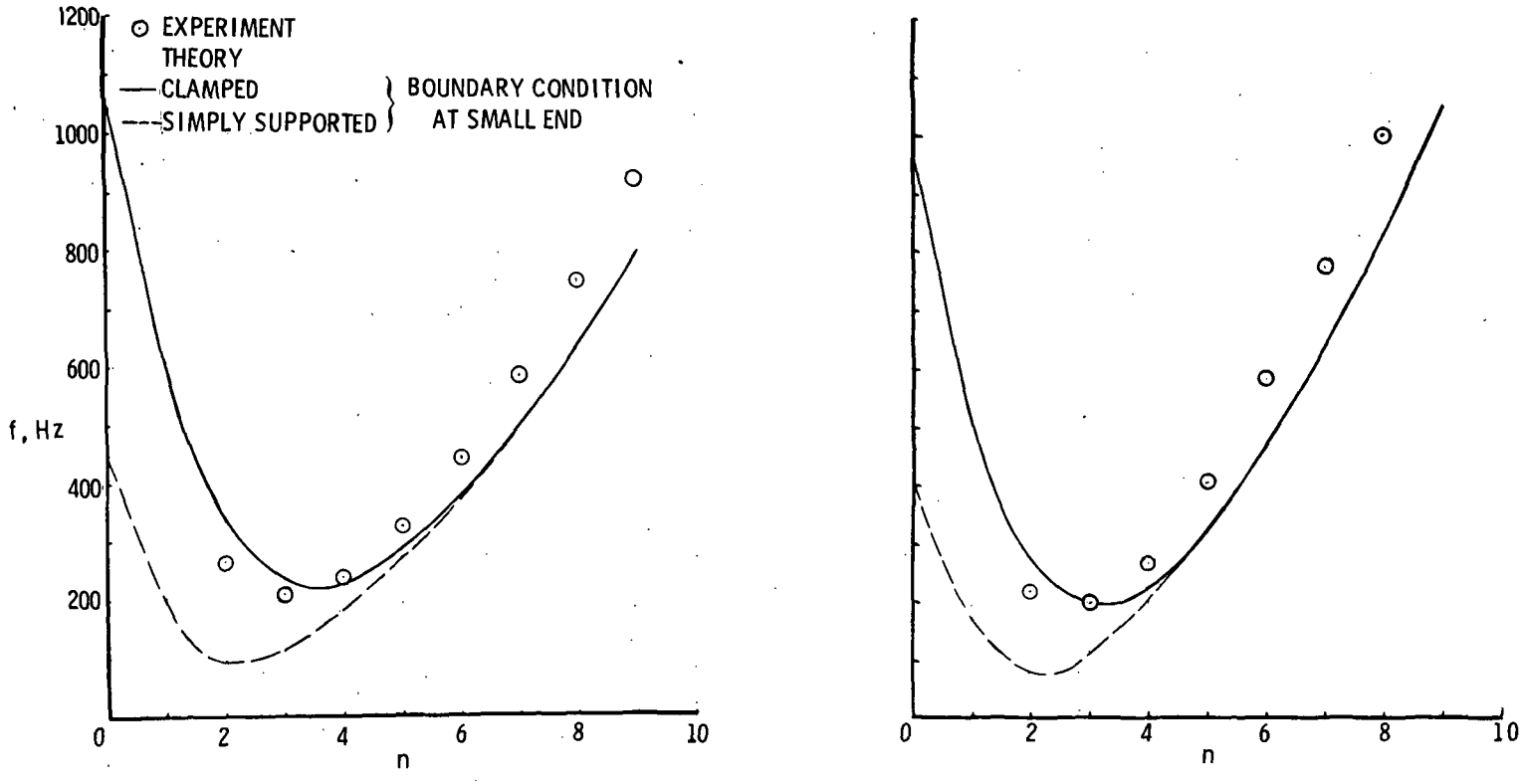

(a) No ring.

(b) d = 0.318 cm (0.125 in.).

Figure 5.- Experimental and theoretical frequencies of the 0.20-cm-thick (0.080-in.) shells).

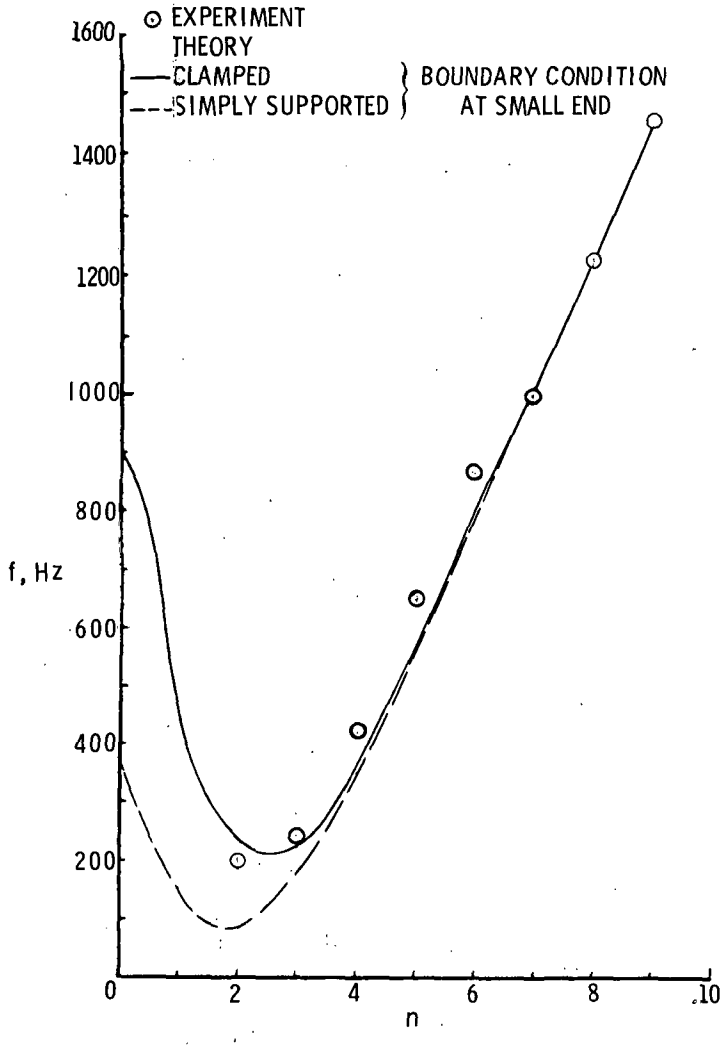

(c) d = 0.635 cm (0.250 in.).

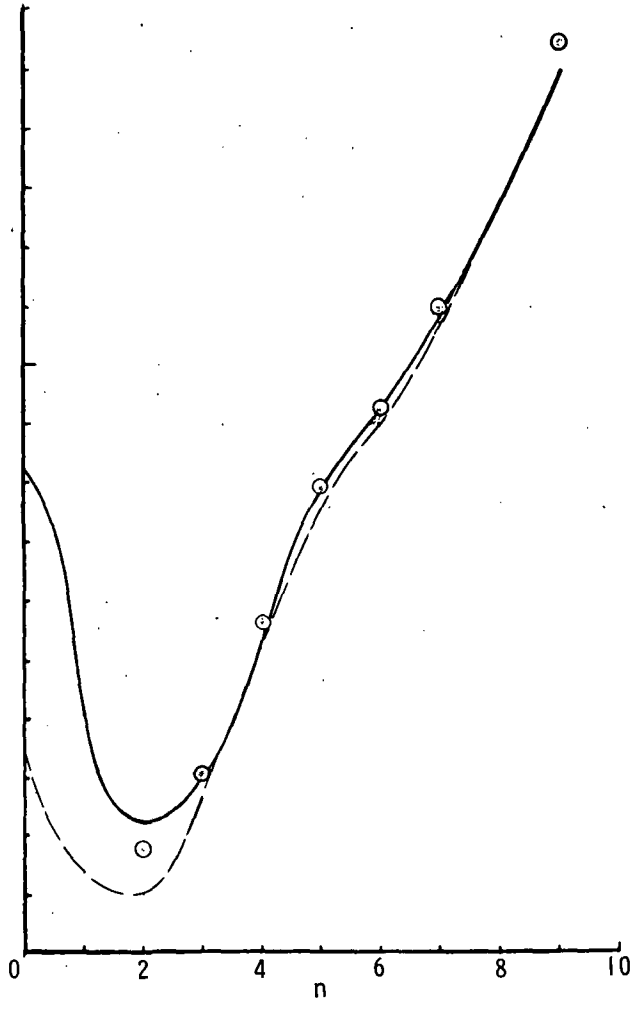

(d) d = 0.953 cm (0.375 in.).

Figure 5.- Continued.

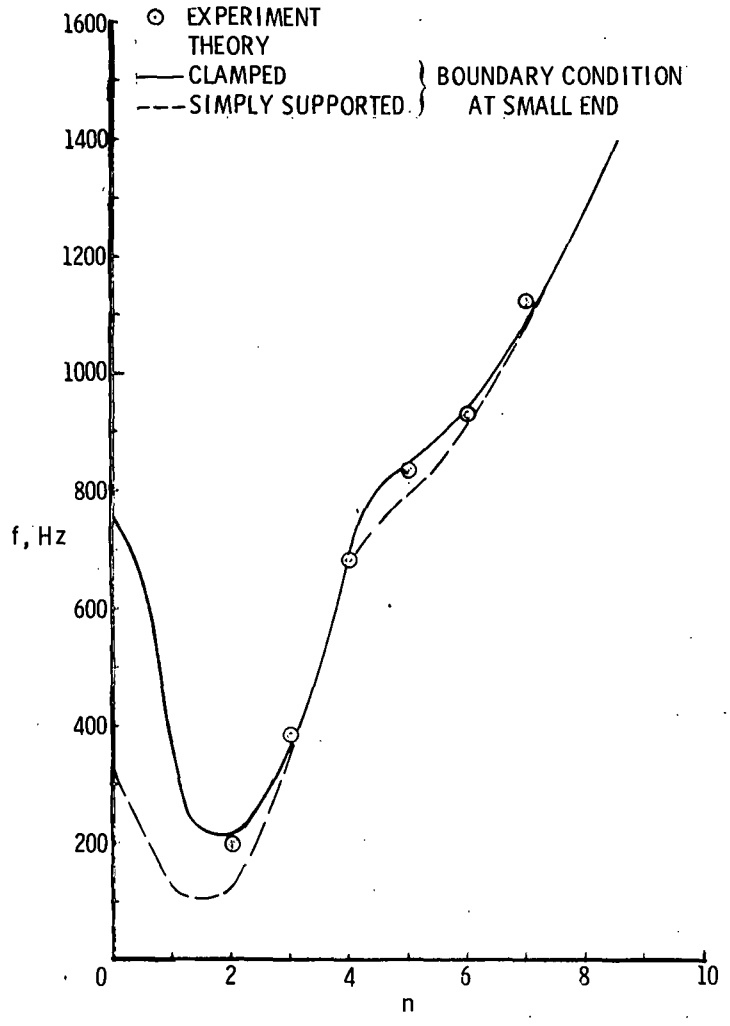

(e) d = 1.27 cm (0.500 in.).

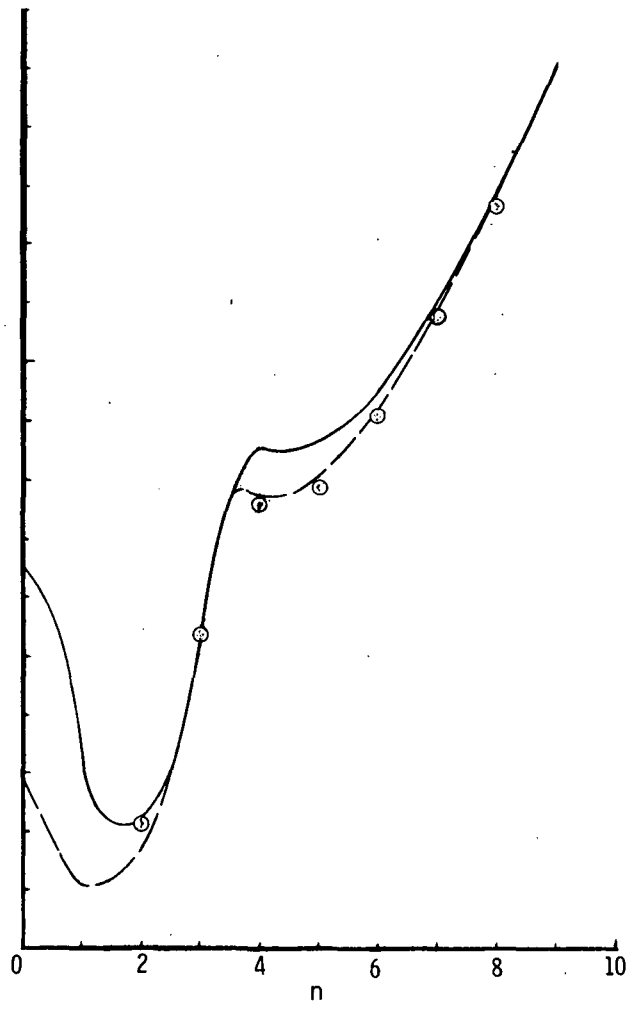

(f) d = 1.91 cm (0.750 in.).

Figure 5.- Continued.

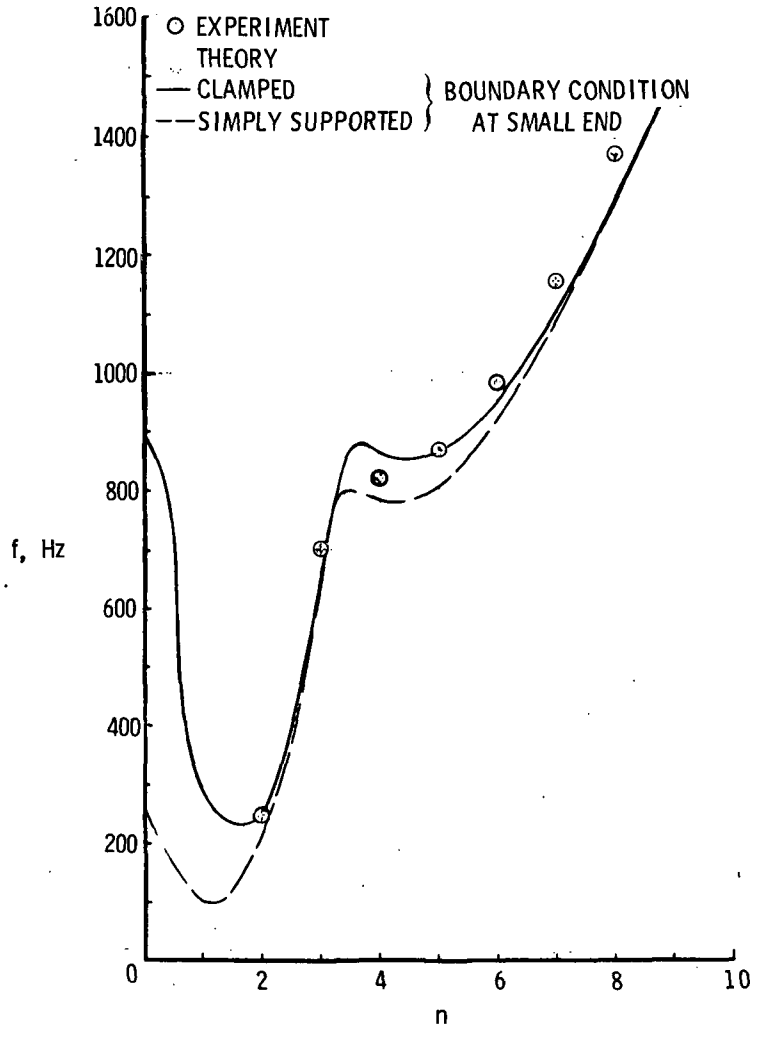

(g) d = 2.54 cm (1.000 in.).

Figure 5.- Concluded.

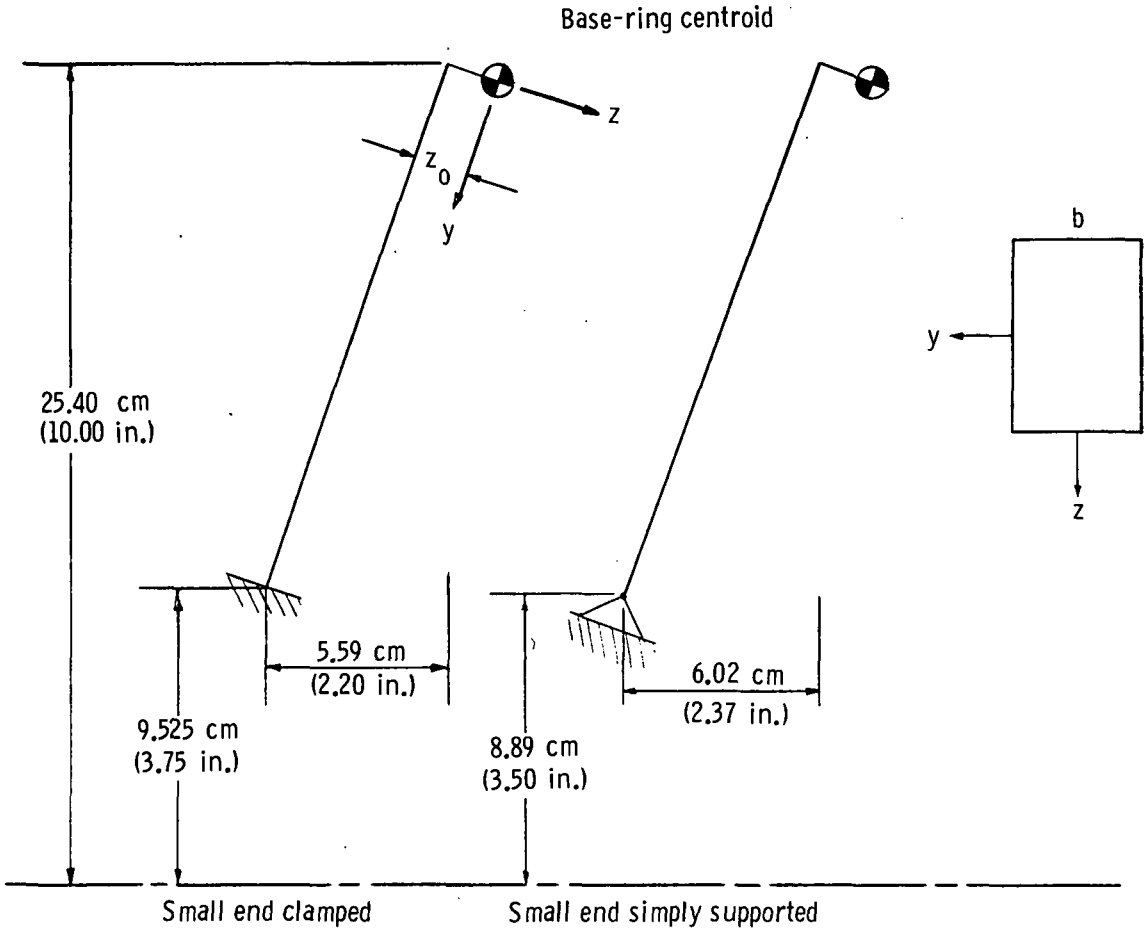

Ring properties

$A = bd$

$I_y = bd^3/12$

$I_z = db^3/12$

$I_{yz} = 0$

$J = \beta db^3$, $b > d$

$J = \beta bd^3$, $b < d$

$z_o = d/2$

b>d		d>b	
b/d	β	d/b	β
5.00	0.29	1.20	0.16
2.50	.25	1.60	.20
1.67	.20		
1.25	.17		

Figure 6.- Idealized shell configuration and ring properties used in theoretical calculations.

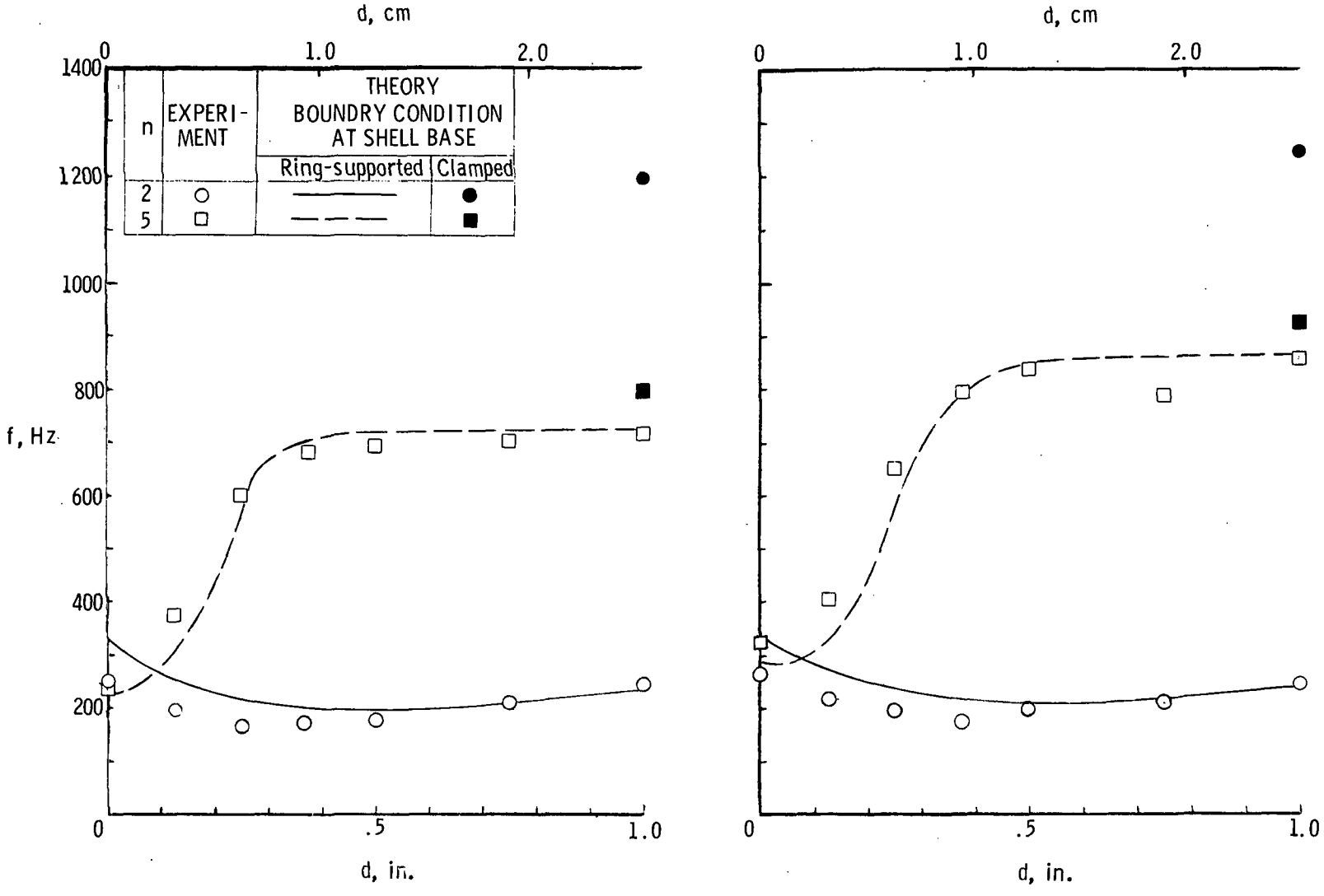

(a) h = 0.152 cm (0.060 in.).

(b) h = 0.203 cm (0.080 in.).

Figure 7.- Effects of base rings on frequency for representative modes.

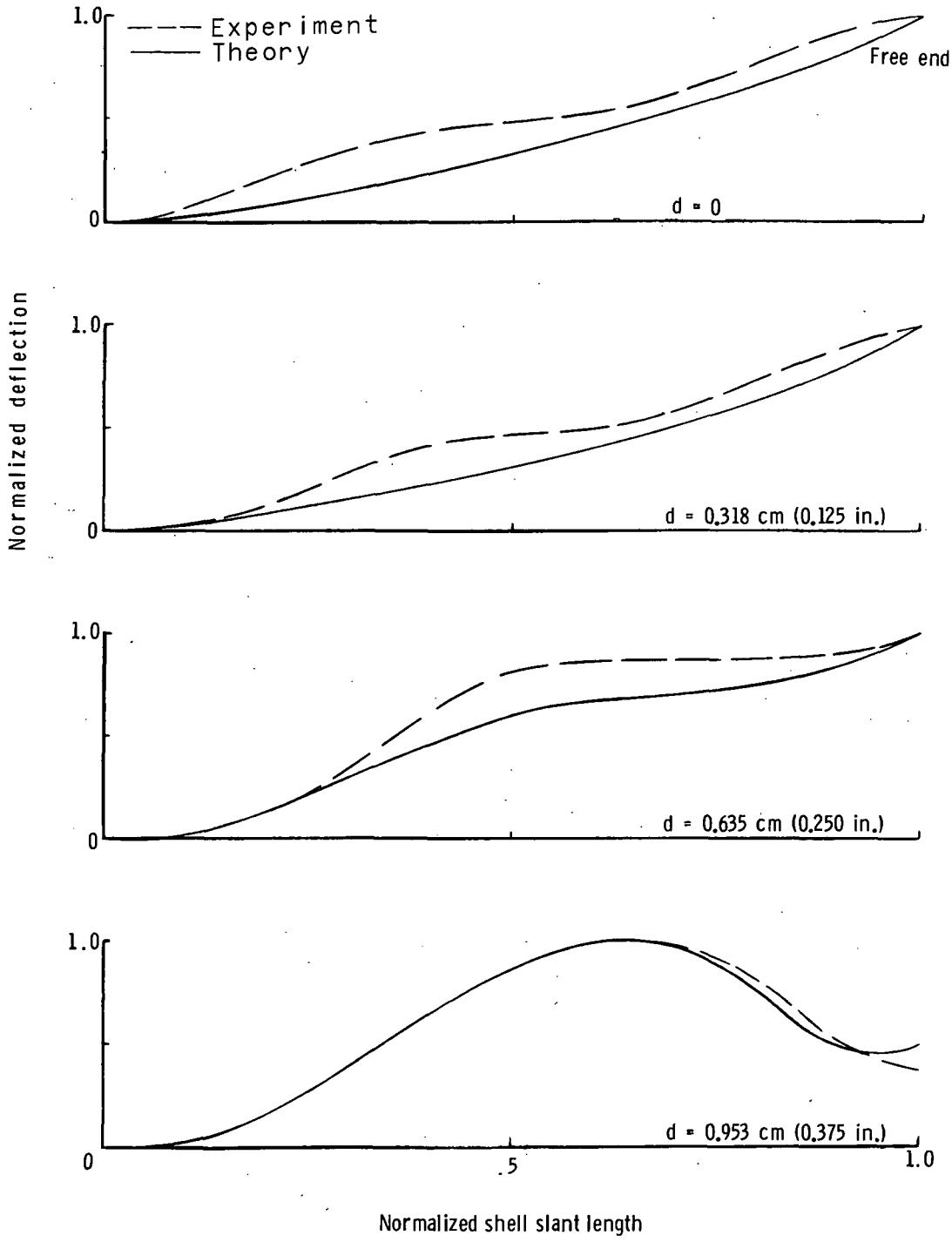

Figure 8.- Effects of base rings on vibration mode shapes for n = 5 and h = 0.203 cm (0.080 in.).

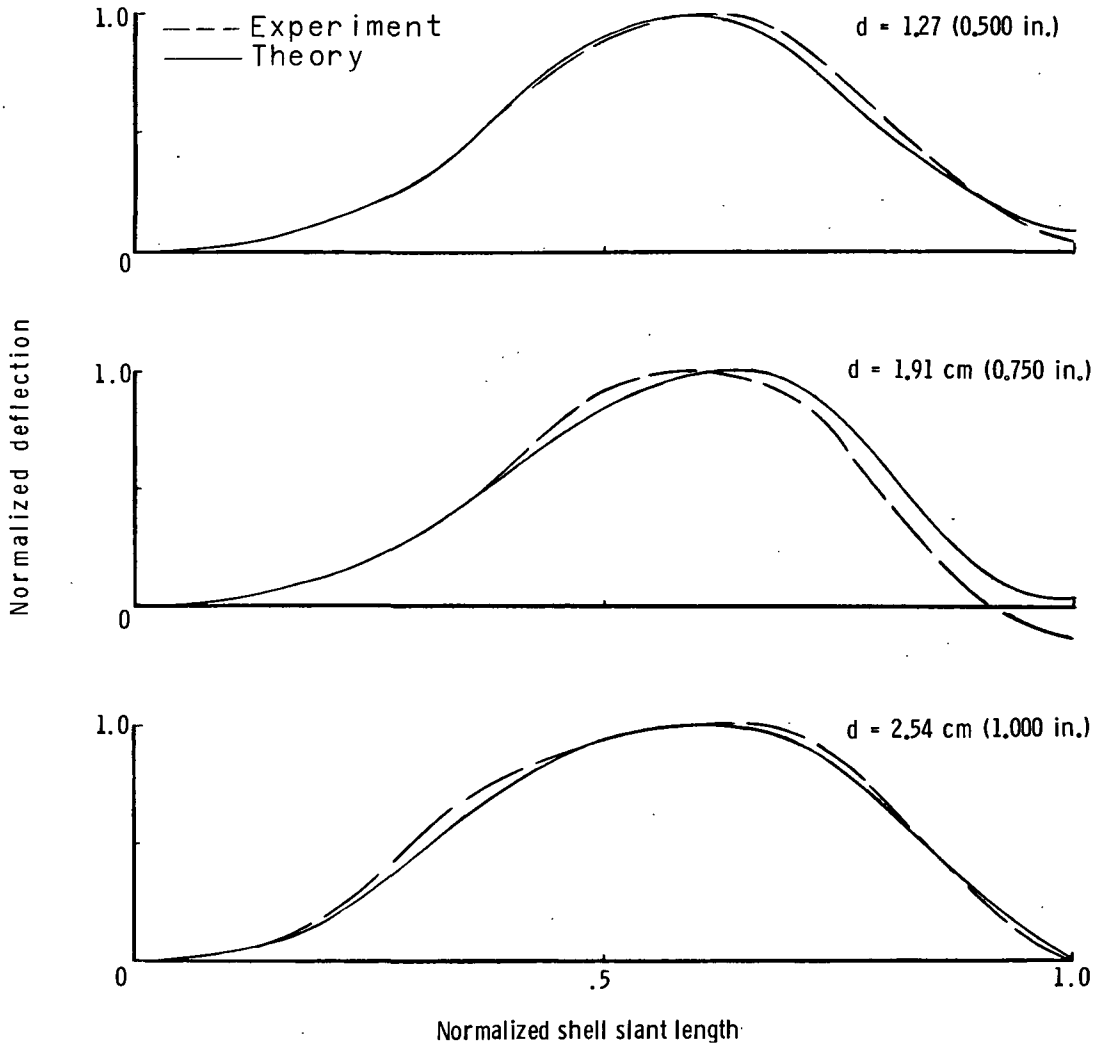

Figure 8.- Concluded.

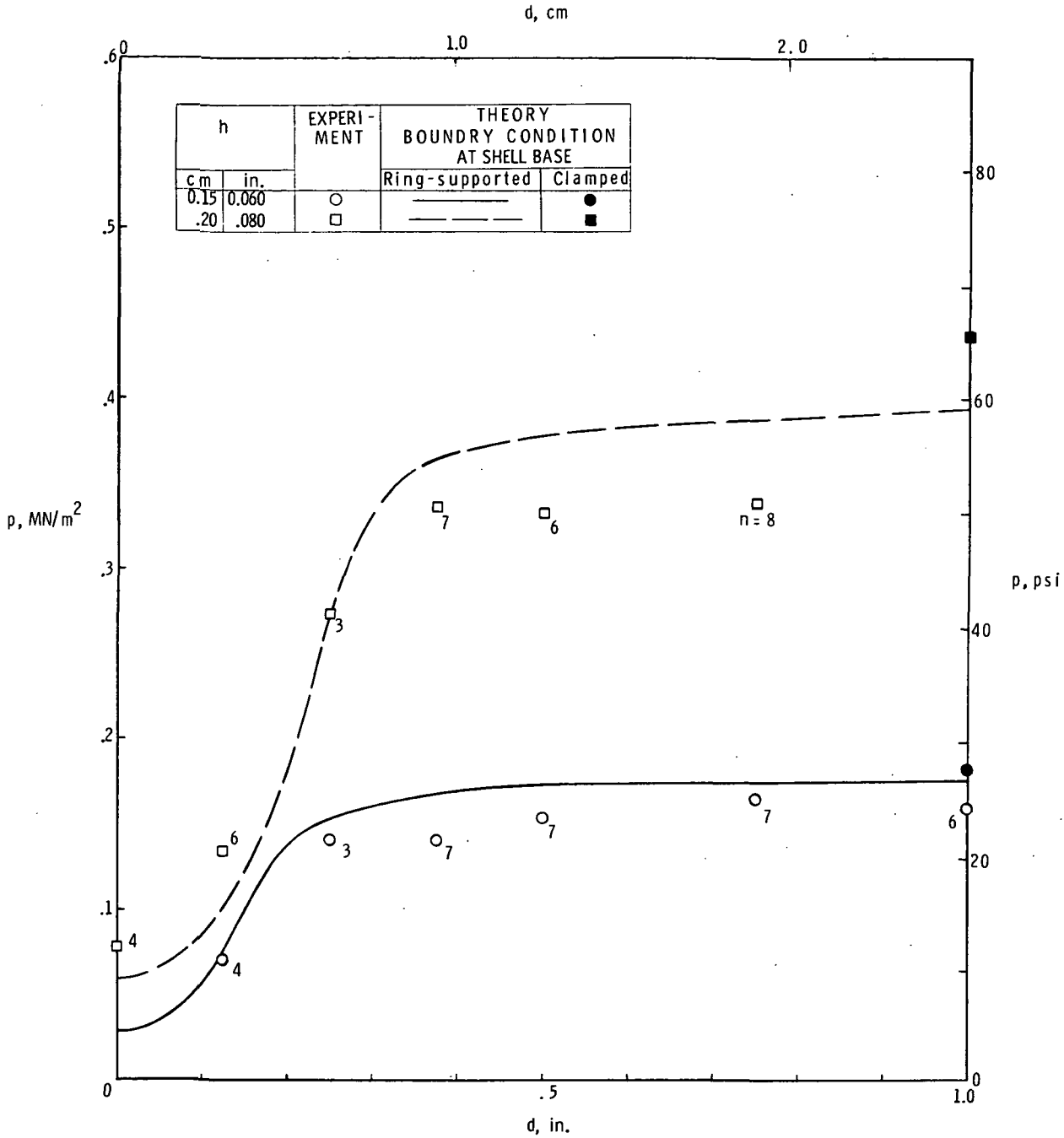

Figure 9.- Effect of base rings on the buckling pressure.

"The aeronautical and space activities of the United States shall be conducted so as to contribute . . . to the expansion of human knowledge of phenomena in the atmosphere and space. The Administration shall provide for the widest practicable and appropriate dissemination of information concerning its activities and the results thereof."

— NATIONAL AERONAUTICS AND SPACE ACT OF 1958

NASA SCIENTIFIC AND TECHNICAL PUBLICATIONS

TECHNICAL REPORTS: Scientific and technical information considered important, complete, and a lasting contribution to existing knowledge.

TECHNICAL NOTES: Information less broad in scope but nevertheless of importance as a contribution to existing knowledge.

TECHNICAL MEMORANDUMS: Information receiving limited distribution because of preliminary data, security classification, or other reasons.

CONTRACTOR REPORTS: Scientific and technical information generated under a NASA contract or grant and considered an important contribution to existing knowledge.

TECHNICAL TRANSLATIONS: Information published in a foreign language considered to merit NASA distribution in English.

SPECIAL PUBLICATIONS: Information derived from or of value to NASA activities. Publications include conference proceedings, monographs, data compilations, handbooks, sourcebooks, and special bibliographies.

TECHNOLOGY UTILIZATION PUBLICATIONS: Information on technology used by NASA that may be of particular interest in commercial and other non-aerospace applications. Publications include Tech Briefs, Technology Utilization Reports and Technology Surveys.

Details on the availability of these publications may be obtained from:

SCIENTIFIC AND TECHNICAL INFORMATION OFFICE

NATIONAL AERONAUTICS AND SPACE ADMINISTRATION

Washington, D.C. 20546